

## Aluminum Hydroxide Secondary Building Units in a Metal-Organic Framework Support Earth-Abundant Metal Catalysts for Broad Scope Organic Transformations

Xuanyu Feng, Pengfei Ji, Zhe Li, Tasha Drake, Pau Oliveres,  
Emily Y Chen, Yang Song, Cheng Wang, and Wenbin Lin

*ACS Catal.*, **Just Accepted Manuscript** • DOI: 10.1021/acscatal.9b00259 • Publication Date (Web): 06 Mar 2019

Downloaded from <http://pubs.acs.org> on March 9, 2019

### Just Accepted

“Just Accepted” manuscripts have been peer-reviewed and accepted for publication. They are posted online prior to technical editing, formatting for publication and author proofing. The American Chemical Society provides “Just Accepted” as a service to the research community to expedite the dissemination of scientific material as soon as possible after acceptance. “Just Accepted” manuscripts appear in full in PDF format accompanied by an HTML abstract. “Just Accepted” manuscripts have been fully peer reviewed, but should not be considered the official version of record. They are citable by the Digital Object Identifier (DOI®). “Just Accepted” is an optional service offered to authors. Therefore, the “Just Accepted” Web site may not include all articles that will be published in the journal. After a manuscript is technically edited and formatted, it will be removed from the “Just Accepted” Web site and published as an ASAP article. Note that technical editing may introduce minor changes to the manuscript text and/or graphics which could affect content, and all legal disclaimers and ethical guidelines that apply to the journal pertain. ACS cannot be held responsible for errors or consequences arising from the use of information contained in these “Just Accepted” manuscripts.



# Aluminum Hydroxide Secondary Building Units in a Metal-Organic Framework Support Earth-Abundant Metal Catalysts for Broad Scope Organic Transformations

Xuanyu Feng,<sup>†,1</sup> Pengfei Ji,<sup>†,1</sup> Zhe Li,<sup>†,1,2</sup> Tasha Drake,<sup>1</sup> Pau Oliveres,<sup>1</sup> Emily Y. Chen,<sup>1</sup> Yang Song,<sup>1</sup> Cheng Wang,<sup>2</sup> and Wenbin Lin<sup>\*,1,2</sup>

<sup>1</sup>Department of Chemistry, The University of Chicago, 929 E 57<sup>th</sup> St, Chicago, IL 60637, USA

<sup>2</sup>College of Chemistry and Chemical Engineering, iCHEM, State Key Laboratory of Physical Chemistry of Solid Surface Xiamen University, Xiamen 361005, China

**ABSTRACT:** The intrinsic heterogeneity of alumina (Al<sub>2</sub>O<sub>3</sub>) surface presents a challenge for the development of alumina-supported single-site heterogeneous catalysts and hinders the characterization of catalytic species at the molecular level as well as the elucidation of mechanistic details of the catalytic reactions. Here we report the use of aluminum hydroxide secondary building units (SBUs) in the MIL-53(Al) metal-organic framework (MOF) with the formula Al( $\mu_2$ -OH)(BDC) (BDC = 1,4-benzenedicarboxylate) as a uniform and structurally-defined functional mimic of Al<sub>2</sub>O<sub>3</sub> surface for supporting Earth-abundant metal (EAM) catalysts. The  $\mu_2$ -OH groups in MIL-53(Al) SBUs were readily deprotonated and metalated with CoCl<sub>2</sub> and FeCl<sub>2</sub> to afford MIL-53(Al)-CoCl and MIL-53(Al)-FeCl precatalysts which were characterized by powder X-ray diffraction, nitrogen sorption, elemental analysis, density functional theory, and extended X-ray fine structure spectroscopy. Activation with NaBEt<sub>3</sub>H converted MIL-53(Al)-CoCl to MIL-53(Al)-CoH which effectively catalyzed hydroboration of alkynes and nitriles and hydrosilylation of esters. X-ray photoelectron spectroscopy and X-ray absorption near-edge spectroscopy (XANES) indicated the presence of Al<sup>3+</sup> and Co<sup>2+</sup> centers in MIL-53(Al)-CoH while deuterium labeling studies suggested  $\sigma$ -bond metathesis as a key step for the MIL-53(Al)-CoH catalyzed addition reactions. MIL-53(Al)-FeCl competently catalyzed oxidative C<sub>sp</sub><sup>3</sup>-H amination and Wacker-type alkene oxidation. XANES analysis revealed the oxidation of Fe<sup>2+</sup> to Fe<sup>3+</sup> centers in the activated MIL-53(Al)-FeCl catalyst and suggested that oxidative C<sub>sp</sub><sup>3</sup>-H amination occurs via the formation of Fe<sup>III</sup>-O<sup>t</sup>Bu species by single electron transfer between Fe<sup>II</sup> centers in MIL-53(Al)-FeCl and (<sup>t</sup>BuO)<sub>2</sub> with concomitant generation of one equiv of <sup>t</sup>BuO<sup>•</sup> radical, C-H activation through hydrogen atom abstraction to generate alkyl radicals, protonation of Fe<sup>III</sup>-O<sup>t</sup>Bu by aniline to generate MIL-53(Al)-Fe<sup>III</sup>-anilide, and finally C-N coupling between the Fe<sup>III</sup>-anilide and alkyl radical to form the Csp<sup>3</sup>-H amination product and regenerate the Fe<sup>II</sup> catalyst. These highly active single-site MOF-based solid catalysts were readily recovered and reused up to five times without significant decrease in catalytic activity. This work thus demonstrates the great potential of using the aluminum hydroxide SBUs in MOFs to support EAM catalysts for important organic transformations.

**KEYWORDS:** Metal-Organic Framework; Earth-Abundant Metal Catalyst; Single-site Solid Catalyst; Hydrofunctionalization; C-H Amination; Wacker-Type Alkene Oxidation

## INTRODUCTION

As one of the most abundant, widely used, and thoroughly studied metal oxide supports, alumina (Al<sub>2</sub>O<sub>3</sub>), especially  $\gamma$ -Al<sub>2</sub>O<sub>3</sub>, has drawn great interest in industrial research studies, due to its high surface area (80-250 m<sup>2</sup>/g), acid/base chemistry, thermal and chemical stability, and abundance of surface hydroxy (OH) groups.<sup>1-4</sup> Previous studies have demonstrated the ability of  $\gamma$ -Al<sub>2</sub>O<sub>3</sub> in supporting either metallic nanoparticles for catalytic methanation<sup>5-7</sup> and dehydrogenation reactions<sup>8-10</sup> or organometallic species for olefin polymerization,<sup>11-12</sup> C-H activation,<sup>13-15</sup> and metathesis reactions.<sup>16-18</sup> However, unlike the thermodynamically stable phase  $\alpha$ -Al<sub>2</sub>O<sub>3</sub>, which has a compact and crystalline structure,  $\gamma$ -Al<sub>2</sub>O<sub>3</sub> features different aluminum (Al) coordination numbers (Al<sub>IV</sub> and Al<sub>VI</sub>) and varied surface OH coordination modes (terminal-,  $\mu_2$ -, and  $\mu_3$ -) to the Al centers (Figure 1a).<sup>1, 4</sup> This intrinsic heterogeneity of  $\gamma$ -Al<sub>2</sub>O<sub>3</sub> surface presents a challenge for the uniform modification of catalytically active species, the characterization of these active species, and the elucidation of reaction mechanisms.<sup>19</sup> Furthermore, non-uniform OH groups and

defect surface Al sites cause undesired reforming and hydration/dehydration process particularly at elevated temperatures,<sup>3</sup> leading to insufficient binding strength between active species and oxide support and consequently decreased catalytic activity. Thus, new Al-based materials with uniform OH groups are highly desired for mimicking  $\gamma$ -Al<sub>2</sub>O<sub>3</sub> in supporting single-site catalysts and providing better understanding of  $\gamma$ -Al<sub>2</sub>O<sub>3</sub>-supported commercial catalytic systems.

Constructed from metal cluster secondary building units (SBUs) and organic linkers, MOFs have provided a unique and highly tunable platform for supporting active species.<sup>20-24</sup> Benefitting from large pore/channel sizes, thermal stability, and predictable structures, MOF-based materials have out-performed traditional heterogeneous catalysts in both activity and selectivity in a number of reactions.<sup>25-32</sup> Moreover, the isolation of active sites in MOFs provides unique opportunities to obtain solution-inaccessible molecular catalysts in MOF structures.<sup>33-36</sup> The inorganic nodes of many MOFs feature functional OH groups to provide a mimic of

metal oxides/hydroxides. The crystallinity of MOF frameworks and the homogeneity of SBUs render the OH groups unique supports for metal complexes to afford single-site solid catalysts. In particular, recent works have demonstrated the anchoring of Earth-abundant metal (EAM) species to Zr-oxo/hydroxo and Ti-oxo/hydroxo SBUs to provide novel single-site solid catalysts for a number of important organic transformations and the control of catalytic activity and selectivity by fine-tuning electronic and steric properties of SBUs.<sup>37-40</sup> SBU-supported single-site EAM catalysts thus present a cost-effective and sustainable strategy for the development of solid catalysts with well-defined catalytic species for the synthesis of commodity and fine chemicals.

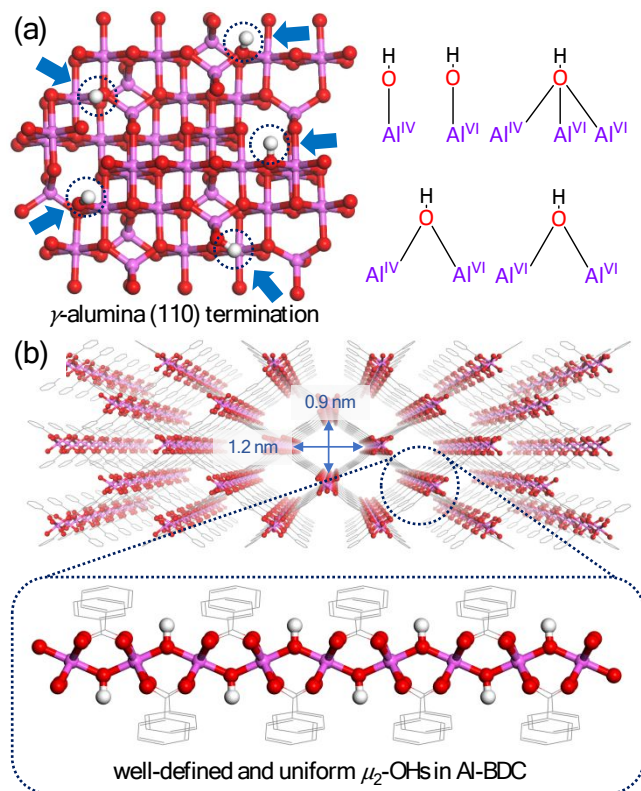


**Figure 1.** (a) The presence of five main types of OH groups on the (110) surface of  $\gamma$ - $\text{Al}_2\text{O}_3$ . (IV and VI stand for coordination numbers of 4 and 6 for Al sites.) (b) The structure of MIL-53(Al) features large one-dimensional channels ( $1.2 \times 0.9 \text{ nm}^2$ ) and a high density of uniform  $\mu_2$ -OH groups.

Herein, we report the use of MIL-53(Al), which is composed of one-dimensional Al-hydroxo chains linked together by 1,4-benzenedicarboxylate (BDC) bridging ligands,<sup>41</sup> as a mimic for the alumina surface to anchor Co and Fe complexes for a broad range of organic transformations. The isolated  $\mu_2$ -OH groups were first deprotonated to give  $\mu_2\text{-O}^-$  and then metalated with Co and Fe complexes to afford MIL-53(Al)-supported precatalysts. Following activation with a hydride source, the resultant MIL-53(Al)-CoH effectively catalyzed hydroboration of alkynes and

nitriles as well as hydrosilylation of esters. MIL-53(Al)-FeCl efficiently catalyzed oxidative C-H amination and Wacker-type alkene oxidation reactions. MIL-53(Al) possesses several advantages over traditional alumina supports including a higher Al to OH ratio (1:1), uniform and structurally defined  $\mu_2$ -OH groups, and all  $\mu_2$ -OH groups being accessible via the porous MOF structure (Figure 1b), allowing for a greater density of functionalization with metal complexes and easier investigation of catalytically active sites and reaction mechanisms. Compared to commonly studied divalent Zn, Cd, and Cu MOFs, Al-based MOFs feature higher thermal stability (over 500 °C) due to the stronger coordination of Al to carboxylate linkers.<sup>42-45</sup> The perforated structure of uniform 1-D channels in MIL-53(Al) allows for facile substrate diffusion to access the catalytic sites to effect reduction and oxidation reactions with diverse mechanisms. Moreover, compared to the well-studied  $\text{Zr}_3\text{-OH}$  sites,  $\text{Al}_2\text{-OH}$  moieties are expected to be more electron donating after deprotonation. MIL-53(Al)-supported EAM catalysts thus represent a versatile and cost-effective alternative to traditional metal oxide heterogeneous catalysts.

## RESULT AND DISCUSSION

### Synthesis and Characterization of MIL-53(Al)-CoCl and MIL-53(Al)-FeCl

MIL-53(Al) with the formula  $\text{Al}(\text{OH})(\text{BDC})$  was synthesized in 85% yield through a solvothermal reaction between  $\text{AlCl}_3 \cdot 6\text{H}_2\text{O}$  and  $\text{H}_2\text{BDC}$  in *N,N*-dimethylformamide (DMF) in 18 h (Figure S1, SI). The previous synthesis of MIL-53(Al) from  $\text{Al}(\text{NO}_3)_3 \cdot 9\text{H}_2\text{O}$  and  $\text{H}_2\text{BDC}$  in  $\text{H}_2\text{O}$  led to trapping of  $\text{H}_2\text{BDC}$  in the MOF channels via H-bonding between free ligands and bridging  $\mu_2$ -OH groups,<sup>41</sup> likely due to the insolubility of  $\text{H}_2\text{BDC}$  in water. In contrast, thermal gravimetric analysis (TGA) results and FT-IR spectra indicated that MIL-53(Al) synthesized from  $\text{AlCl}_3 \cdot 6\text{H}_2\text{O}$  in DMF are free of trapped  $\text{H}_2\text{BDC}$  and features open channels and uniform free  $\mu_2$ -OH groups for anchoring catalytically active metal centers (Figure S2, S3, SI).<sup>46</sup> MIL-53(Al) was first treated with  $\text{LiCH}_2\text{Si}(\text{CH}_3)_3$  to generate  $\text{Al}(\text{OLi})(\text{BDC})$  via deprotonation, and then metalated with 1 equiv. of  $\text{CoCl}_2$  or  $\text{FeCl}_2$ . After removing unreacted metal salts via extensive washing with tetrahydrofuran (THF), MIL-53(Al)-CoCl and MIL-53(Al)-FeCl were obtained as light blue and light brown solids, respectively. Powder X-ray diffraction (PXRD) patterns of the metalated MOFs remained unchanged from that of as-synthesized MIL-53(Al), indicating the maintenance of crystallinity after metalation with Co and Fe (Figure 2b). The Co and Fe contents in the metalated MOFs were determined to be 0.15 Co per Al and 0.23 Fe per Al, respectively, by inductively coupled plasma-mass spectrometry (ICP-MS) analysis of digested samples. Nitrogen sorption isotherms of MIL-53(Al)-CoCl and MIL-53(Al)-FeCl indicated highly porous structures with Brunauer-Emmett-Teller (BET) surface areas 2066 and 2001  $\text{m}^2/\text{g}$ , respectively (Figure 2c). Pore size distribution analyses by density functional theory (DFT) showed a pore size of 8 Å for both metalated MOFs, matching well with that expected from the crystal structure (Figure 2d).

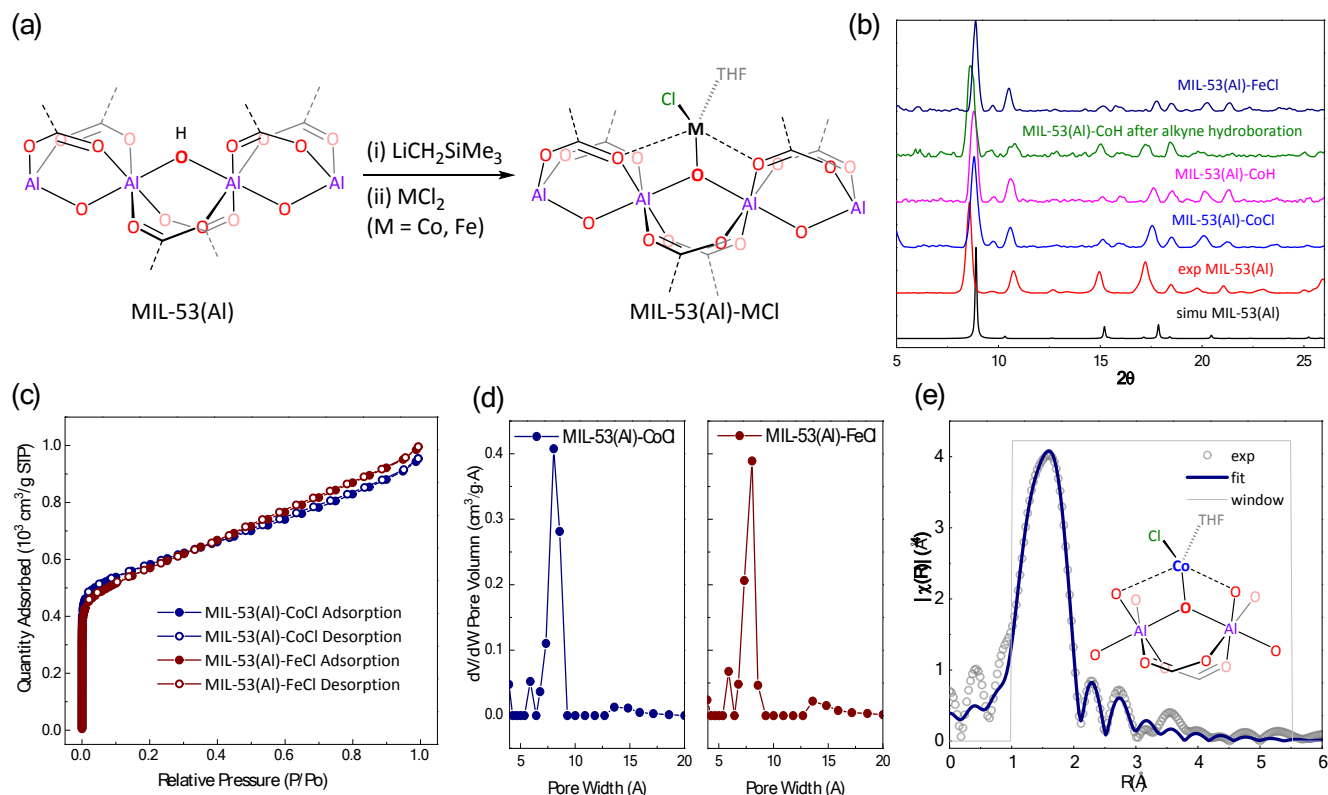


**Figure 2.** (a) The preparation of MIL-53(Al)-CoCl from MIL-53(Al) via sequential deprotonation and metalation. (b) PXRD patterns of as-synthesized MIL-53(Al) (red), MIL-53(Al)-CoCl (blue), MIL-53(Al)-FeCl (navy), indicating that crystallinity of the MOF was maintained after metalation. PXRD patterns of MIL-53(Al)-CoH (magenta) and after catalytic alkyne hydroboration are unchanged from that of MIL-53(Al)-CoCl, indicating the MOF is stable toward activation and under catalytic reactions. (c) N<sub>2</sub> sorption isotherms of MIL-53(Al)-CoCl (navy) and MIL-53(Al)-FeCl (wine). (d) Pore size distributions of MIL-53(Al)-CoCl (navy) and MIL-53(Al)-FeCl (wine), both showing a uniform pore size of 8 Å. (e) EXAFS spectra (gray circles) and fits (navy solid line) in R-space at the Co K-edge adsorption of MIL-53(Al)-CoCl. The Co coordination mode was calculated by DFT.

We performed DFT calculations using the B3LYP level of theory to optimize the coordination environments of Co and Fe in metalated MOFs. The Co coordination converged at a distorted square pyramidal geometry with one anionic bridging oxo (from the deprotonation of the  $\mu_2$ -OH group), two carboxylate oxygen, one chloride, and one THF molecule to afford the  $[(\mu_2\text{-O})(\text{carboxylate-O})_2\text{CoCl}(\text{THF})]$  species. The Co- $(\mu_2\text{-O})$  distance is 1.91 Å, while the Co-(carboxylate-O) distances are longer at 2.21 Å and 2.58 Å, respectively. The Co-Cl distance is 2.33 Å and the Co-(THF-O) distance is 2.06 Å (Table S4, SI). The calculated model fitted well to the Co K-edge absorption of the extended X-ray fine structure spectroscopy (EXAFS) data of MIL-53(Al)-CoCl with a R factor of 0.0045 (Figure 2e, Table S1, SI). EXAFS fitting gave a Co- $(\mu_2\text{-O})$  distance of 1.87 Å, and Co-(carboxylate-O) distances of 1.96 Å and 2.32 Å, a Co-Cl distance of 2.28 Å, and a Co-(THF-O) distance of 2.02 Å. DFT calculations indicated a similar distorted square pyramidal geometry for Fe centers in MIL-53(Al)-FeCl. The calculated Fe- $(\mu_2\text{-O})$  distance of 1.91 Å, Fe-(carboxylate-O) distances of 2.32 and 2.41 Å, Fe-Cl distance of 2.31 Å, and Fe-(THF-O) distance of 2.14 Å (Table S6, SI) match well with those determined by EXAFS fitting (1.91, 2.39, 2.48, 2.13, and 2.11 Å, respectively). The R-factor of the EXAFS fitting is 0.015 (Figure S14, Table S3, SI).

#### Structure and Electronic Properties of MIL-53(Al)-CoH

Upon treatment with NaBEt<sub>3</sub>H, the color of MIL-53(Al)-CoCl changed from light blue to black, suggesting the formation of MIL-53(Al)-CoH via chloride/hydride exchange. The MOF crystallinity was maintained after chloride/hydride exchange based on the

similarity of PXRD patterns. X-ray photoelectron spectroscopy (XPS) was used to determine the oxidation states of Al and Co centers in MIL-53(Al)-CoH. MIL-53(Al)-CoH displayed strong 2p<sub>3/2</sub> and 2p<sub>1/2</sub> peaks at 778.3 and 794.3 eV along with strong 2p<sub>3/2</sub> and 2p<sub>1/2</sub> shake-up peaks at 783.0 and 800.2 eV for Co centers, indicating typical Co<sup>II</sup> species (Figure 3d). MIL-53(Al)-CoH showed one set of strong 2p<sub>3/2</sub> and 2p<sub>1/2</sub> peaks at 71.5 and 71.0 eV for Al centers, which are characteristic of Al<sup>III</sup> species (Figure 3e). These results indicate that neither Al<sup>III</sup> or Co<sup>II</sup> species were reduced by NaBEt<sub>3</sub>H during the chloride/hydride exchange process.

X-ray absorption near-edge spectroscopy (XANES) analysis supported the Co oxidation state assignment by XPS. The pre-K edge features of MIL-53(Al)-CoCl and MIL-53(Al)-CoH are identical to that of CoCl<sub>2</sub>, indicating the Co<sup>2+</sup> centers before and after chloride/hydride exchange (Figure 3c). The presence of only Co<sup>2+</sup> centers in MIL-53(Al)-CoH ruled out the possibility of forming Co nanoparticle during the NaBEt<sub>3</sub>H treatment. The absence of Co nanoparticle was also supported by the significant misfit of MIL-53(Al)-CoH EXAFS data using a model containing 5% of Co nanoparticle (Figure S11, SI). Treatment of MIL-53(Al)-CoH with excess amount of trifluoroacetic acid (TFA) generated 1.10±0.03 equiv. of H<sub>2</sub> w.r.t. Co, indicating the presence of Co-H species in the MOF (Figure S12, SI). EXAFS fitting was also performed at the Co K-edge for MIL-53(Al)-CoH. The EXAFS spectrum was well fitted with a Co coordination environment calculated by DFT, indicating the formation of  $(\mu_2\text{-O})(\text{O-carboxylate})_2\text{CoH}(\text{THF})$  species in MIL-53(Al)-CoH (Figure 3b and Table S2, SI).

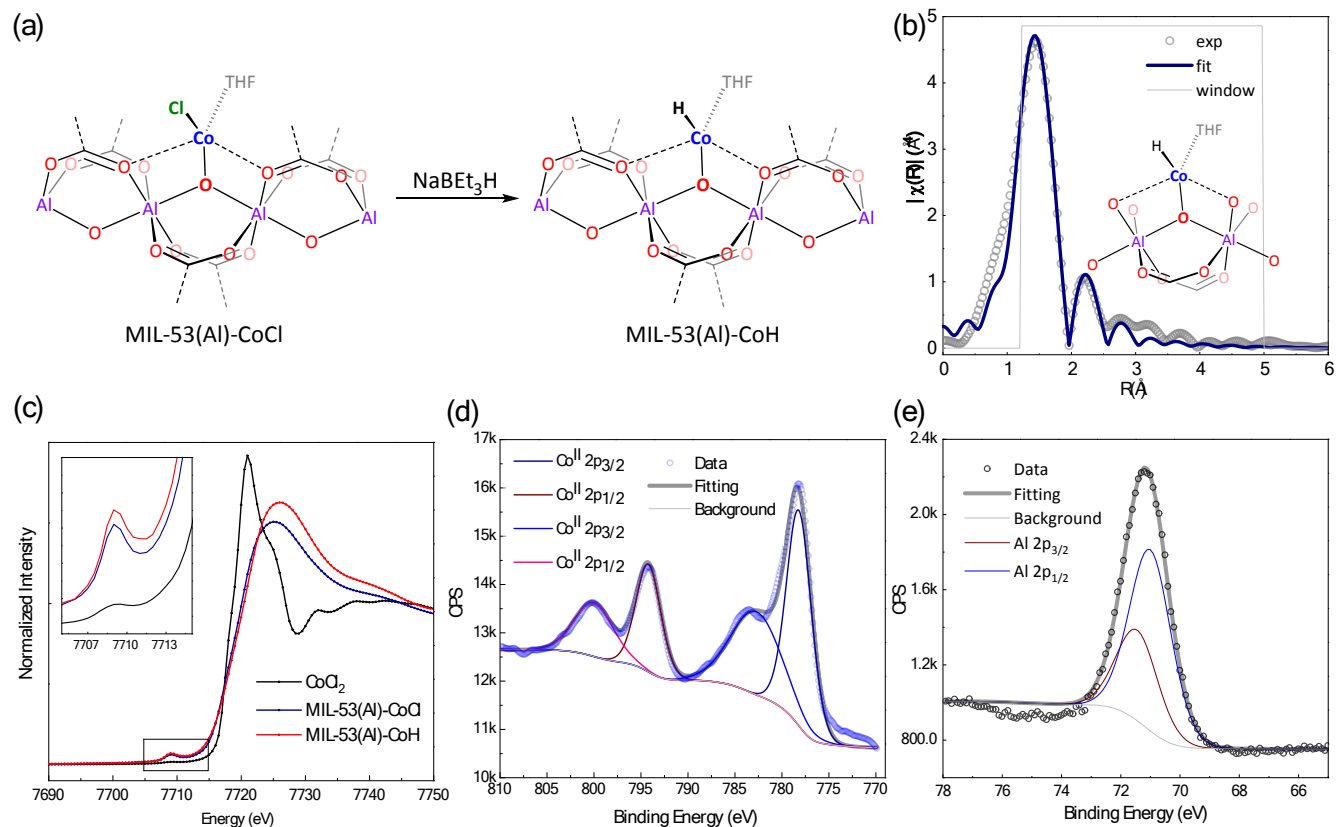


**Figure 3.** (a) Activation of MIL-53(Al)-CoCl to form MIL-53(Al)-CoH with NaBEt<sub>3</sub>H in THF. (b) EXAFS fitting of MIL-53(Al)-CoH shows the Co coordination environment as ( $\mu_2$ -O)(O-carboxylate)<sub>2</sub>CoH(THF). (c) XANES pre-edge features of MIL-53(Al)-CoCl (navy) and MIL-53(Al)-CoH (red) as compared to that of CoCl<sub>2</sub> (black), indicating the Co<sup>2+</sup> oxidation state before and after NaBEt<sub>3</sub>H treatment. (d) Co 2p XPS spectra of MIL-53(Al)-CoH (blue circle) and the fitting result (gray solid line) indicate the Co<sup>2+</sup> oxidation state after NaBEt<sub>3</sub>H treatment. (e) Al 2p XPS spectra of MIL-53(Al)-CoH (black circle) and fitting result (gray solid line) indicate the Al<sup>3+</sup> oxidation state after NaBEt<sub>3</sub>H treatment.

### MIL-53(Al)-CoH Catalyzed Hydroboration of Alkynes

Alkenylboronate esters are important starting materials for the synthesis of a wide range of organic compounds via cross-coupling reactions.<sup>47-49</sup> Transition metal catalyzed hydroboration of alkynes provides the simplest and most atom-efficient synthetic route to alkenylboronate esters.<sup>50-53</sup> Several complexes of EAMs, *e.g.*, Fe,<sup>54-56</sup> Co,<sup>57-58</sup> and Cu,<sup>59-60</sup> have recently been shown to catalyze hydroboration of alkynes, but these reactions either require high catalyst loadings or the use of additives.

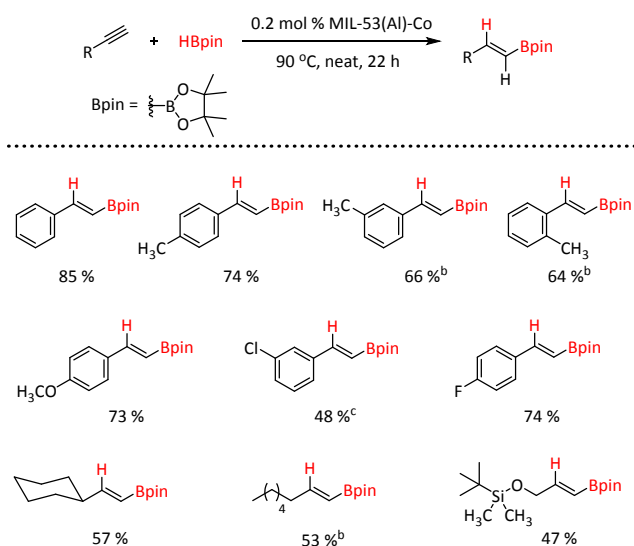
MIL-53(Al)-CoH was found to be a highly effective catalyst for hydroboration of alkynes. Screening of reaction conditions (Table S7, SI) revealed that, at 0.2 mol% of catalyst loading, MIL-53(Al)-CoH catalyzed the solvent-free reaction of phenylacetylene with 1.2 equiv pinacolborane (HBpin) at 90 °C for 22 h to give the *E*-alkenylboronate in 85% yield, with a turnover number (TON) of 425. No conversion was found in the control experiment without adding the MOF. Addition of 2 equiv. HBpin did not lead to further hydroboration of the alkenylboronate ester. A TON of 1428 was achieved when the reaction was carried out with 0.035 mol % MIL-53(Al)-CoH at 90 °C (Table S7, SI). PXRD pattern of MIL-53(Al)-CoH recovered from the hydroboration reaction was similar to that of as-synthesized MIL-53(Al)-CoH (Figure 2b), indicating the stability of MOF framework during hydroboration reaction.

MIL-53(Al)-CoH-catalyzed hydroboration has a broad substrate scope and exhibits good functional group tolerance. (Table 1) Both electron donating group (*i.e.*, CH<sub>3</sub>, OCH<sub>3</sub>) and electron withdrawing group (*i.e.*, F) work well under standard reaction conditions. The methyl group on the *para* position did not impact

the reactivity, but the substrates with the methyl group in *ortho* and *meta* positions required twice the catalyst loading. Halogen atoms did not interfere with the hydroboration reaction. Under unoptimized conditions, MIL-53(Al)-CoH catalyzed hydroboration of aliphatic alkynes to give exclusively *E*-alkenylboronate esters in 47-57% of yields.

As a solid catalyst, MIL-53(Al)-CoH was readily recycled and re-used for hydroboration of phenylacetylene. At a 1.0 mol% Co loading, MIL-53(Al)-Co catalyzed five consecutive runs of phenylacetylene hydroboration without a significant drop in yields (Figure S23, SI). The leaching of Co and Al into the supernatant after the hydroboration was determined to be 0.3% and 0.8%, respectively, by ICP-MS analysis. Moreover, control experiments using Co nanoparticles with the same amount of Co gave very low yields of the products (Table S8, SI), further confirming single-site supported Co-H complex as the true catalytic species.

**Table 1.** MIL-53(Al)-CoH catalyzed hydroboration of alkynes<sup>a</sup>

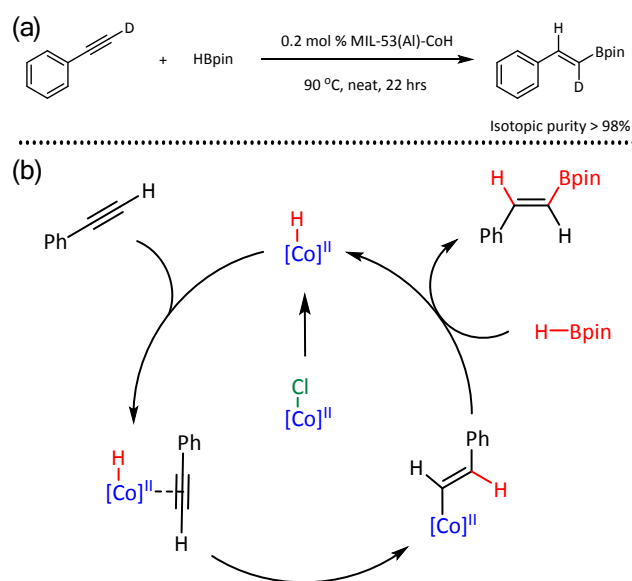


17  
18  
19  
20

<sup>a</sup>Standard condition: 1.00 mmol alkyne substrate, 1.20 mmol HBpin, 0.2 mol% Co, 90 °C, 22 h; Yield was determined by <sup>1</sup>H NMR using mesitylene as internal standard. <sup>b</sup>0.4 mol% Co. <sup>c</sup>1.0 mol% Co.

21  
22  
23  
24  
25  
26  
27  
28  
29  
30  
31  
32  
33  
34

We also conducted deuterium labeling experiments to gain further insight into MIL-53(Al)-Co catalyzed hydroboration of alkynes. After hydroboration of phenylacetylene-*d*<sub>1</sub> with HBpin, <sup>1</sup>H NMR analysis of the product (53% yield) revealed exclusive deuterium labeling at the 1-position of trans-2-phenylvinylboronic acid pinacol ester (Figure 4a), indicating no H/D exchange between the alkyne and Co centers.<sup>61</sup> Based on the deuterium labeling result and the Co<sup>2+</sup> oxidation state in 53(Al)-CoH, we propose a reaction pathway involving  $\sigma$ -bond metathesis as a key step for the hydroboration of terminal alkynes (Figure 4b). The coordination of an alkyne to the Co center of the active catalyst MIL-53(Al)-CoH is followed by migratory insertion of the hydride to the triple bond to form the Co-alkenyl intermediate, which undergoes  $\sigma$ -bond metathesis with HBpin to give the alkenylboronate ester product and regenerate the Co-H catalyst (Figure 4b).



53  
54  
55

**Figure 4.** (a) Deuterium labeling experiment and (b) proposed mechanism of MIL-53(Al)-CoH catalyzed hydroboration of alkynes.

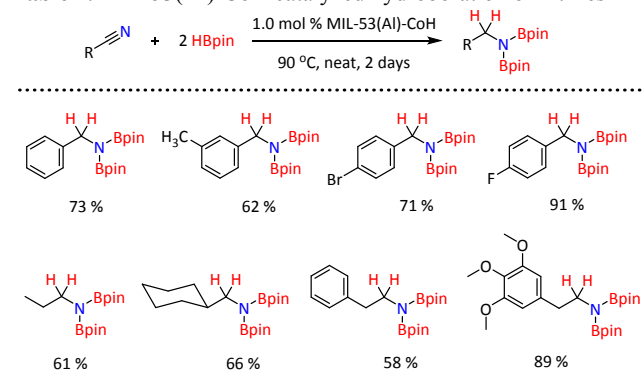
#### MIL-53(Al)-CoH Catalyzed Hydroboration of Nitriles

56  
57  
58  
59  
60

Encouraged by the success in hydroboration of alkynes, we tested

MIL-53(Al)-CoH in hydroboration of nitriles. Reduction of nitriles to amines with high activity and selectivity is important for the production of many dyes, agrochemicals, and pharmaceutical compounds.<sup>62</sup> Hydroboration of nitriles also provides a route to protected amines for further functionalization.<sup>63-65</sup> Treatment of benzonitrile with 2.1 equiv. of HBpin in the presence of 1.0 mol% MIL-53(Al)-CoH at 90 °C for 2 days afforded the fully hydroborated product in 73% yield. No semi-hydroborated or other by-products were observed. Under this un-optimized condition, a wide range of nitriles were hydroborated with HBpin to afford fully hydroborated products in 58% to 91% yields (Table 2). The hydroboration reaction works for aromatic nitriles containing electron-withdrawing groups, electron-donating groups, and halogens as well as aliphatic nitriles (Table 2).

**Table 2.** MIL-53(Al)-CoH catalyzed hydroboration of nitriles<sup>a</sup>



<sup>a</sup>Standard condition: 0.60 mmol nitrile, 1.26 mmol HBpin, 1.0 mol% Co, 90 °C, 2 days; Yield was determined by <sup>1</sup>H NMR using mesitylene as internal standard.

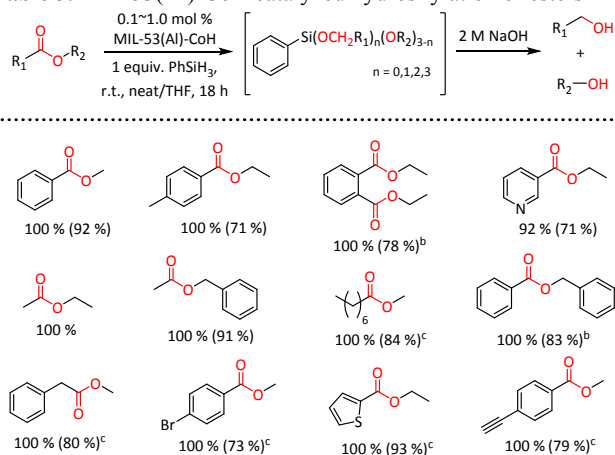
#### MIL-53(Al)-CoH Catalyzed Hydrosilylation of Esters

Beside hydroboration reactions, hydrosilylation provides another reductive pathway to introduce silyl groups into unsaturated bonds for further functionalization.<sup>66-68</sup> In contrast to extensively studied hydrosilylation of ketones and aldehydes,<sup>69-73</sup> hydrosilylation of less reactive substrates such as amides and esters remains a challenge, especially for EAM catalysts.<sup>74-76</sup> We investigated hydrosilylation of esters using MIL-53(Al)-CoH as catalyst. Impressively, at 0.1 mol% loading of the MOF catalyst, simply stirring an equimolar mixture of methyl benzoate and phenylsilane (PhSiH<sub>3</sub>) at room temperature over 18 h afforded the hydrosilylation products with complete conversion. <sup>1</sup>H NMR spectroscopy identified the hydrosilylation products as a mixture of PhSi(OCH<sub>3</sub>)<sub>2</sub>(OCH<sub>2</sub>C<sub>6</sub>H<sub>5</sub>) (42 mol%), PhSi(OCH<sub>3</sub>)(OCH<sub>2</sub>C<sub>6</sub>H<sub>5</sub>)<sub>2</sub> (45 mol%), and PhSi(OCH<sub>2</sub>C<sub>6</sub>H<sub>5</sub>)<sub>3</sub> (13 mol%) in addition to the by-product PhSi(OCH<sub>3</sub>)<sub>3</sub>. Treatment of this mixture with 2 M NaOH in 1:1 MeOH/H<sub>2</sub>O (v/v) afforded benzyl alcohol in 92% isolated yield. No conversion was observed in the background reaction without the MOF catalyst.

MIL-53(Al)-CoH catalyzed hydrosilylation of esters exhibited a broad substrate scope. (Table 3) Substituted benzoates, dibenzoates, and acetate esters were readily hydrosilylated in the presence of 0.1 mol% MIL-53(Al)-CoH. For less reactive aliphatic esters, such as methyl octanoate and methyl phenylacetate, quantitative hydrosilylation was achieved in the presence of 1.0 mol% MIL-53(Al)-CoH. Due to the mild reaction conditions, MIL-53(Al)-CoH catalyzed hydrosilylation showed good functional group tolerance to esters containing reducible groups such as alkynyl and bromo groups. More importantly, MIL-53(Al)-CoH catalyzed hydrosilylation of esters containing a pyridyl or thiophenyl moiety, which usually poisons catalysts due to strong coordination to the metal centers. Upon basic workup,

corresponding alcohols were obtained in 71% and 93% yield.

**Table 3.** MIL-53(Al)-CoH catalyzed hydrosilylation of esters<sup>a</sup>



<sup>a</sup> Standard condition: 1.0 mmol ester, 1.0 mmol PhSiH<sub>3</sub>, 0.1-1.0 mol% Co, r.t., 18 h; For solid substrates, 0.3 mL THF was added as solvent; Hydrosilylation yields are based on <sup>1</sup>H NMR integration with isolated yields of alcohols in parenthesis. <sup>b</sup>0.5 mol% Co. <sup>c</sup>1.0 mol% Co.

### MIL-53(Al)-FeCl Catalyzed C-H Amination

To further explore the potential of MIL-53(Al) hydroxyl groups as a support for base metal catalysts, we introduced Fe centers into this MOF. MIL-53(Al)-FeCl was similarly prepared as a pale yellow solid through deprotonation of  $\mu_2$ -OH sites in MIL-53(Al) with LiCH<sub>2</sub>SiMe<sub>3</sub> followed by metalation with FeCl<sub>2</sub>. We hypothesized that the Fe<sup>II</sup> centers can undergo the Fe<sup>II</sup>/Fe<sup>III</sup> redox process to enable the application of MIL-53(Al)-FeCl in catalyzing challenging reactions through single electron transfer (SET) processes.

Catalytic formation of C-N bonds through Csp<sup>3</sup>-H amination using Earth-abundant and environmental friendly first-row transition metals (e.g., Fe, Cu) has attracted significant research interest.<sup>77-79</sup> We tested the catalytic performance of MIL-53(Al)-FeCl in Csp<sup>3</sup>-H amination using aniline as the nitrogen source. At 5.0 mol% loading of MIL-53(Al)-Fe, heating a mixture of aniline and indane in the presence of 1.5 equiv. of (tBuO)<sub>2</sub> at 105 °C gave the desired amination product, N-phenyl-2,3-dihydro-1H-inden-1-amine, in 63% yield. The protocol converted tetralin to the Csp<sup>3</sup>-H amination product in 70% yield. Indane and tetralin were also aminated with different aniline derivatives containing 2,4,6-substituents and 4-substituent to afford desired products in moderate to good yields (15-70% yields for 5 mol% catalyst loading, Table 4). Lower yields of desired Csp<sup>3</sup>-H amination products were obtained for bulky anilines such as 2,4,6-trimethylaniline and 2,4,6-trichloroaniline, likely as a result of steric hindrance around the Fe centers. Higher yields of amination products were generally obtained for *para*-substituted anilines with electron-withdrawing groups (Cl and Br) in comparison with those with electron-donating groups (CH<sub>3</sub>).

MIL-53(Al)-FeCl catalyzed Csp<sup>3</sup>-H amination was proposed to proceed through radical-mediated C-H activation followed by C-N cross coupling between the alkyl radical and Fe<sup>III</sup>-anilide, analogous to the mechanism proposed in the literature for Cu<sup>I</sup>-catalyzed CH amination reactions.<sup>80-81</sup> XANES analysis was carried out to identify the oxidation state of Fe centers in the activated MIL-53(Al)-FeCl catalyst (Figure 5a). As-prepared MIL-53(Al)-FeCl exhibited similar pre-edge features to FeCl<sub>2</sub>. After treatment with (tBuO)<sub>2</sub>, the MOF showed similar pre-edge features to FeCl<sub>3</sub>, indicating the formation of Fe<sup>III</sup>-O<sup>t</sup>Bu species via SET between Fe<sup>II</sup> centers in MIL-53(Al)-FeCl and (tBuO)<sub>2</sub> with

concomitant generation of one equiv of <sup>t</sup>BuO<sup>•</sup> radical. The <sup>t</sup>BuO<sup>•</sup> radical subsequently underwent C-H activation through hydrogen atom abstraction (HAT). Interestingly, Fe<sup>III</sup> pre-edge features of MIL-53(Al)-Fe<sup>III</sup>O<sup>t</sup>Bu were maintained after its treatment with aniline, indicating a simple anion exchange with aniline to generate MIL-53(Al)-Fe<sup>III</sup>-anilide. The final step of the reaction involved C-N coupling between the Fe<sup>III</sup>-anilide and alkyl radical with concomitant SET to the anilide to the Fe<sup>III</sup> center to regenerate the Fe<sup>II</sup> catalyst (Figure 5b).

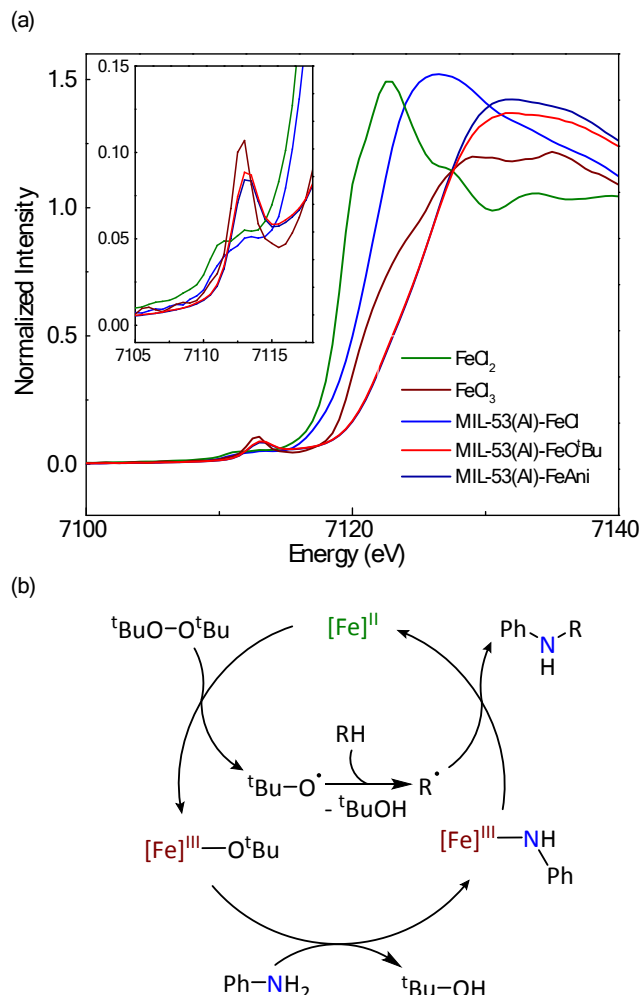
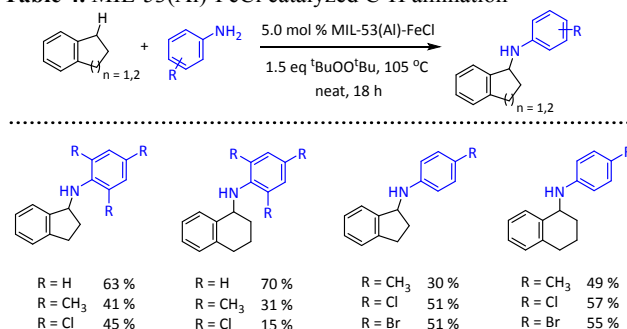


**Figure 5.** (a) XANES pre-edge features of MIL-53(Al)-Fe<sup>II</sup>Cl (blue), MIL-53(Al)-Fe<sup>III</sup>O<sup>t</sup>Bu (red), and MIL-53(Al)-Fe<sup>III</sup>-anilide (navy) as compared to those of FeCl<sub>2</sub> (green) and FeCl<sub>3</sub> (wine). (b) Proposed mechanism for MIL-53(Al)-FeCl catalyzed Csp<sup>3</sup>-H amination involving the Fe<sup>II</sup>/Fe<sup>III</sup> cycle.

**Table 4.** MIL-53(Al)-FeCl catalyzed C-H amination<sup>a</sup>



<sup>a</sup> Standard condition: 0.32 mmol anilines substrate, 6.4 mmol indane or tetralin, 5 mol% Fe, 105 °C, 18 h; Yield was determined by <sup>1</sup>H NMR or

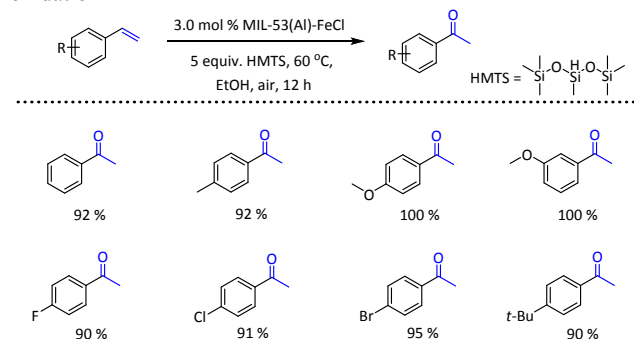
GC-MS analysis using mesitylene as internal standard.

### MIL-53(Al)-FeCl Catalyzed Wacker-Type Alkene Oxidation

MIL-53(Al)-FeCl is also highly effective in catalyzing Wacker-type alkene oxidation reactions. Wacker-Tsuji oxidation directly converts terminal alkenes into carbonyl-containing compounds using a wide range of oxidants.<sup>82-83</sup> However, precious metal catalysts (*e.g.*, PdCl<sub>2</sub>) along with stoichiometric Cu salt<sup>83-85</sup> or “unusual” oxidants, such as hypervalent iodine<sup>86</sup> and 1,4-benzoquinoline,<sup>87-88</sup> are needed in Wacker oxidation reactions to achieve high chemo-selectivity, significantly restricting their broad applications. Recently, Han and co-workers<sup>89</sup> reported an Fe-based catalyst for Wacker-type oxidation under ambient air conditions. The reaction was believed to go through the Fe<sup>II</sup>/Fe<sup>III</sup> cycle. We hypothesized that MIL-53(Al) with isolated  $\mu_2$ -OH sites could provide an excellent support for developing single-site solid catalyst for Wacker-type olefin oxidation.

After screening different silanes and reaction temperatures (Table S9, SI), we found that MIL-53(Al)-FeCl showed high catalytic activity for the oxidation of a wide range of styrene derivatives using ambient air as the oxidant and 1,1,1,3,5,5,5-heptamethyltrisiloxane (HMTS) as the additive. (Table 5) At 3.0 mol% loading of MIL-53(Al)-FeCl (*w.r.t.* Fe), acetophenone was obtained in 92% yield from the oxidation of styrene at 60 °C for 12 h. No reaction occurred in the absence of either the MOF, silanes, or the air (Table S9, SI). Substrate scope of this reaction was broad and extended to styrenes containing both electron-donating groups such as methyl, methoxyl (at either *para*- or *meta*-position), and *t*-butyl groups and electron-withdrawing groups such as fluoro, chloro, and bromo substituents. In all cases, acetophenone derivatives were obtained in very high yields (90-100%). MIL-53(Al)-FeCl was also readily recovered and used in three consecutive run of oxidation reactions with no significant drop in reaction yields (Figure S44, SI). Only 0.3% of Fe leached into the supernatant as determined by ICP-MS, indicating the stability of the MOF catalyst.

**Table 5.** MIL-53(Al)-FeCl catalyzed Wacker-type alkene oxidation<sup>a</sup>



<sup>a</sup> Standard condition: 0.20 mmol alkenes substrate, 1.0 mmol HMTS, 3 mol% Fe, 1.0 mL dry EtOH, 60 °C, 12 h; Yield was determined by GC-MS analysis using mesitylene as internal standard.

### Catalytic Performance Comparison between MIL-53(Al)-CoH and UiO-68-CoH

To further demonstrate the outstanding catalytic performance and the unique electronic property of EAM catalysts supported on Al-OH chain SBUs, several control reactions were conducted using the well-established UiO-68-Co MOF catalyst at the same Co loading.<sup>28</sup> Significantly lower yields of hydroboration and hydrosilylation products were observed when UiO-68-CoH was used in place of MIL-53(Al)-CoH. For the hydroboration of

alkynes, aromatic alkynes (phenylacetylene) and aliphatic alkynes (ethynylcyclohexane) achieved moderate to good yields at 0.2 mol% MIL-53(Al)-CoH loading, but the same loading of UiO-68-CoH afforded the aromatic and aliphatic products in 16% and 8% yields, respectively. Significant drops of catalytic activities were also observed in the hydroboration of aromatic and aliphatic nitriles. Moreover, UiO-68-CoH was completely inactive for the hydrosilylation of esters, with >99% of starting substrates recovered (Figure 6).

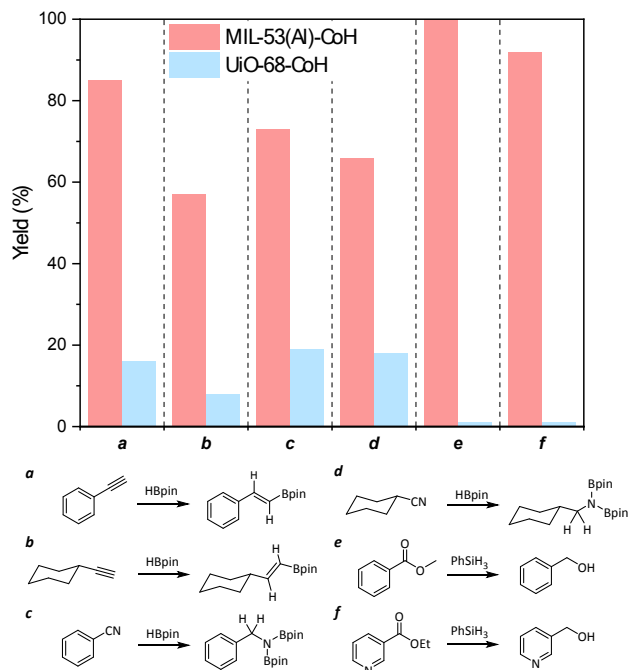


**Figure 6.** Hydroboration of alkynes and nitriles and hydrosilylation of esters with different MOF SBU supported Co-hydride catalysts. Reaction conditions: *a,b*) 0.2 mol% of MOF-CoH catalyst, alkynes (1.0 mmol), HBpin (1.2 mmol), 90 °C, 22 h. *c,d*) 1.0 mol% of MOF-CoH catalyst, nitriles (0.6 mmol), HBpin (1.26 mmol), 90 °C, 2 days. *e,f*) 0.1 mol% of MOF-CoH catalyst, esters (1.0 mmol), PhSiH<sub>3</sub> (1.0 mmol), *r.t.*, 18 h.

To understand the reason for such drastic differences in hydrofunctionalization activities, DFT calculations were carried out on the two MOF SBU supported Co-hydride catalytic systems. With the same overall charge and Co<sup>II</sup> spin state, MIL-53(Al)-CoH features a more electron-rich hydride site with a NBO charge of -0.441 on the hydride. In comparison, UiO-68-CoH has a NBO charge of -0.354 on the hydride (Figure 7, Table S11, S12). We believe that electron-rich oxo sites in MIL-53(Al)-CoH afford a reactive Co-hydride for insertion to the unsaturated bonds to lead to excellent catalytic performance in hydrofunctionalization reactions. Upon dissociation of THF, the Co centers in MIL-53(Al)-CoH also have more open coordination site for substrate binding to further facilitate hydrofunctionalization reactions.

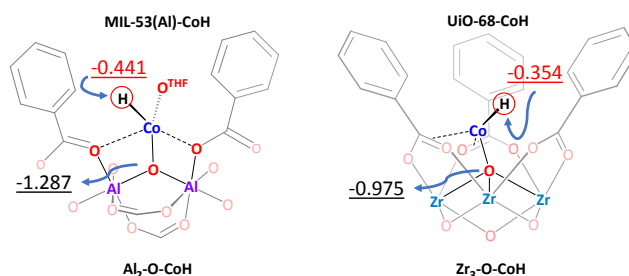


**Figure 7.** NBO charges of Co centers and hydride and bridging oxo groups in MIL-53(Al)-CoH and UiO-68-CoH.

## CONCLUSION

MIL-53(Al) with one-dimensional Al-OH chain SBUs was used as a structural and functional mimic of  $\gamma$ -Al<sub>2</sub>O<sub>3</sub> surface to support Earth-abundant Co and Fe catalysts. Deprotonation of the  $\mu_2$ -OH groups in MIL-53(Al) followed by metalation with CoCl<sub>2</sub> and FeCl<sub>2</sub> afforded MIL-53(Al)-CoCl and MIL-53(Al)-FeCl precatalysts which showed impressive catalytic activities in distinct reductive addition and oxidative amination/alkene oxidation reactions. MIL-53(Al)-CoCl was activated by NaBEt<sub>3</sub>H to afford MIL-53(Al)-CoH for reductive hydrofunctionalization reactions, including hydroboration of alkynes to generate *E*-alkenylboronates, hydroboration of nitriles to give *N,N*-difunctionalized amines, and hydrosilylation of esters followed by hydrolysis to afford corresponding alcohols. Due to the site-isolation effect and unique coordination environment, this highly stable and solution-inaccessible Co<sup>II</sup> hydride species exhibits unprecedented catalytic activities in reductive hydrofunctionalization reactions. On the other hand, due to the Fe<sup>II</sup>/Fe<sup>III</sup> redox property, MIL-53(Al)-FeCl catalyzed interesting oxidative transformations, including Csp<sup>3</sup>-H amination and Wacker-type alkene oxidation reactions. Spectroscopic studies indicated the involvement of the Fe<sup>II</sup>/Fe<sup>III</sup> redox process in oxidative transformations. Compared to traditional  $\gamma$ -Al<sub>2</sub>O<sub>3</sub>-supported metal catalysts, structurally-defined and single-site of MIL-53(Al)-M (M = Co, Fe) solid catalysts allow for molecular level understanding of coordination environments and electronic structures of the catalytically active site as well as the probing of reaction mechanisms in unprecedented details. Moreover, control experiments combined with computational studies showed that such Al<sub>2</sub>-O<sup>-</sup> sites provide electron-rich Co-H sites to facilitate hydrofunctionalization reactions. The establishment of structure/activity relationships in MOF-supported catalysts promises to facilitate their rational optimization to afford cost-effective and sustainable solid catalysts for the practical synthesis of commodity and fine chemicals.

## ASSOCIATED CONTENT

### Supporting Information

This material is available free of charge via the Internet at <http://pubs.acs.org>. Synthesis and characterization of MIL-53(Al), MIL-53(Al)-CoCl, MIL-53(Al)-CoH and MIL-53(Al)-FeCl; reaction procedure and product characterization of catalytic reactions, including cobalt catalyzed alkyne hydroboration, nitrile hydroboration, ester hydrosilylation, and iron catalyzed C-H amination and alkene oxidation.

## AUTHOR INFORMATION

†X. Feng, P. Ji, and Z. Li contributed equally to this work.

Corresponding Author Email: [wenbinlin@uchicago.edu](mailto:wenbinlin@uchicago.edu)

## ORCID

## ACKNOWLEDGMENT

This work was supported by NSF (CHE-1464941). XAS analysis was performed at Beamline 10-BM, supported by the Materials Research Collaborative Access Team (MRCAT). Use of the Advanced Photon Source, an Office of Science User Facility

operated for the U.S. DOE Office of Science by ANL, was supported by the U.S. DOE under Contract No. DE-AC02-06CH11357. Z. Li acknowledges financial support from the China Scholarship Council and the National Science Foundation of China (21671162).

## References

- (1) Tsyganenko, A. A.; Mardilovich, P. P., Structure of alumina surfaces. *J. Chem. Soc., Faraday Trans.* **1996**, *92*, 4843-4852.
- (2) Euzen, P.; Raybaud, P.; Krokidis, X.; Toulhoat, H.; Le Loarer, J. L.; Jolivet, J. P.; Froidefond, C., Alumina. *Handbook of porous solids* **2002**, 1591-1677.
- (3) Trueba, M.; Trasatti, S. P.,  $\gamma$  - Alumina as a support for catalysts: a review of fundamental aspects. *Eur. J. Inorg. Chem.* **2005**, *2005*, 3393-3403.
- (4) Shirai, T.; Watanabe, H.; Fuji, M.; Takahashi, M., Structural properties and surface characteristics on aluminum oxide powders. **2010**.
- (5) Eckle, S.; Anfang, H.-G.; Behm, R. J., Reaction Intermediates and Side Products in the Methanation of CO and CO<sub>2</sub> over Supported Ru Catalysts in H<sub>2</sub>-Rich Reformate Gases. *J. Phys. Chem. C* **2011**, *115*, 1361-1367.
- (6) Garbarino, G.; Riani, P.; Magistri, L.; Busca, G., A study of the methanation of carbon dioxide on Ni/Al<sub>2</sub>O<sub>3</sub> catalysts at atmospheric pressure. *Int. J. Hydrogen Energy* **2014**, *39*, 11557-11565.
- (7) Zhen, W.; Li, B.; Lu, G.; Ma, J., Enhancing catalytic activity and stability for CO<sub>2</sub> methanation on Ni-Ru/[ $\gamma$ ]-Al<sub>2</sub>O<sub>3</sub> via modulating impregnation sequence and controlling surface active species. *RSC Adv.* **2014**, *4*, 16472-16479.
- (8) Yang, H.; Xu, L.; Ji, D.; Wang, Q.; Lin, L., The Catalytic Dehydrogenation of c<sub>2</sub>h<sub>6</sub> to c<sub>2</sub>h<sub>4</sub> under non-Oxidative Conditions over the 6cr/g-al<sub>2</sub>o<sub>3</sub>Catalyst. *React. Kinet. Catal. Lett.* **2002**, *76*, 151-159.
- (9) Bocanegra, S. A.; Castro, A. A.; Guerrero-Ruiz, A.; Scelza, O. A.; de Miguel, S. R., Characteristics of the metallic phase of Pt/Al<sub>2</sub>O<sub>3</sub> and Na-doped Pt/Al<sub>2</sub>O<sub>3</sub> catalysts for light paraffins dehydrogenation. *Chem. Eng. J.* **2006**, *118*, 161-166.
- (10) Iglesias-Juez, A.; Beale, A. M.; Maaijen, K.; Weng, T. C.; Glatzel, P.; Weckhuysen, B. M., A combined in situ time-resolved UV-Vis, Raman and high-energy resolution X-ray absorption spectroscopy study on the deactivation behavior of Pt and PtSn propane dehydrogenation catalysts under industrial reaction conditions. *J. Catal.* **2010**, *276*, 268-279.
- (11) Motta, A.; Fragalà, I. L.; Marks, T. J., Links Between Single-Site Heterogeneous and Homogeneous Catalysis. DFT Analysis of Pathways for Organozirconium Catalyst Chemisorptive Activation and Olefin Polymerization on  $\gamma$ -Alumina. *J. Am. Chem. Soc.* **2008**, *130*, 16533-16546.
- (12) Williams, L. A.; Marks, T. J., Chemisorption Pathways and Catalytic Olefin Polymerization Properties of Group 4 Mono- and Binuclear Constrained Geometry Complexes on Highly Acidic Sulfated Alumina. *Organometallics* **2009**, *28*, 2053-2061.
- (13) Eisen, M. S.; Marks, T. J., Recent developments in the surface and catalytic chemistry of supported organoactinides. *J. Mol. Catal.* **1994**, *86*, 23-50.
- (14) Joubert, J.; Delbecq, F.; Thieuleux, C.; Taoufik, M.; Blanc, F.; Copéret, C.; Thivolle-Cazat, J.; Basset, J.-M.; Sautet, P., Synthesis, Characterization, and Catalytic Properties of  $\gamma$ -Al<sub>2</sub>O<sub>3</sub>-Supported Zirconium Hydrides through a Combined Use of Surface Organometallic Chemistry and Periodic Calculations. *Organometallics* **2007**, *26*, 3329-3335.
- (15) Delley, M. F.; Silaghi, M.-C.; Nuñez-Zarur, F.; Kovtunov, K. V.; Salnikov, O. G.; Estes, D. P.; Koptug, I. V.; Comas-Vives, A.; Copéret, C., X-H Bond Activation on Cr(III),O Sites (X = R, H):

Key Steps in Dehydrogenation and Hydrogenation Processes. *Organometallics* **2017**, *36*, 234-244.

(16) Mostafa, T.; Erwan, L. R.; Jean, T. C.; Jean - Marie, B., Direct Transformation of Ethylene into Propylene Catalyzed by a Tungsten Hydride Supported on Alumina: Trifunctional Single - Site Catalysis. *Angew. Chem. Int. Ed.* **2007**, *46*, 7202-7205.

(17) Alain, S.; Anne, B.; Jean - Marie, B.; Christophe, C., Tuning the Selectivity of Alumina - Supported (CH<sub>3</sub>)ReO<sub>3</sub> by Modifying the Surface Properties of the Support. *Angew. Chem. Int. Ed.* **2008**, *47*, 2117-2120.

(18) Merle, N.; Stoffelbach, F.; Taoufik, M.; Le Roux, E.; Thivolle-Cazat, J.; Basset, J.-M., Selective and unexpected transformations of 2-methylpropane to 2,3-dimethylbutane and 2-methylpropene to 2,3-dimethylbutene catalyzed by an alumina-supported tungsten hydride. *Chem. Commun.* **2009**, 2523-2525.

(19) Rascón, F.; Wischert, R.; Copéret, C., Molecular nature of support effects in single-site heterogeneous catalysts: silica vs. alumina. *Chem. Sci.* **2011**, *2*, 1449-1456.

(20) Ma, L.; Abney, C.; Lin, W., Enantioselective catalysis with homochiral metal-organic frameworks. *Chem. Soc. Rev.* **2009**, *38*, 1248-1256.

(21) Lee, J.; Farha, O. K.; Roberts, J.; Scheidt, K. A.; Nguyen, S. T.; Hupp, J. T., Metal-organic framework materials as catalysts. *Chem. Soc. Rev.* **2009**, *38*, 1450-1459.

(22) Furukawa, H.; Cordova, K. E.; O'Keeffe, M.; Yaghi, O. M., The Chemistry and Applications of Metal-Organic Frameworks. *Science* **2013**, *341*.

(23) Gu, Z. Y.; Park, J.; Raiff, A.; Wei, Z.; Zhou, H. C., Metal-Organic Frameworks as Biomimetic Catalysts. *ChemCatChem* **2014**, *6*, 67-75.

(24) Zhao, M.; Ou, S.; Wu, C.-D., Porous Metal-Organic Frameworks for Heterogeneous Biomimetic Catalysis. *Acc. Chem. Res.* **2014**, *47*, 1199-1207.

(25) Huang, Y.; Liu, T.; Lin, J.; Lü, J.; Lin, Z.; Cao, R., Homochiral Nickel Coordination Polymers Based on Salen(Ni) Metalloligands: Synthesis, Structure, and Catalytic Alkene Epoxidation. *Inorg. Chem.* **2011**, *50*, 2191-2198.

(26) Manna, K.; Zhang, T.; Greene, F. X.; Lin, W., Bipyridine- and Phenanthroline-Based Metal-Organic Frameworks for Highly Efficient and Tandem Catalytic Organic Transformations via Directed C-H Activation. *J. Am. Chem. Soc.* **2015**, *137*, 2665-2673.

(27) Sawano, T.; Lin, Z.; Boures, D.; An, B.; Wang, C.; Lin, W., Metal-Organic Frameworks Stabilize Mono(phosphine)-Metal Complexes for Broad-Scope Catalytic Reactions. *J. Am. Chem. Soc.* **2016**, *138*, 9783-9786.

(28) Manna, K.; Ji, P.; Lin, Z.; Greene, F. X.; Urban, A.; Thacker, N. C.; Lin, W., Chemoselective single-site Earth-abundant metal catalysts at metal-organic framework nodes. *Nat. Commun.* **2016**, *7*, 12610.

(29) Cheng - Xia, C.; Zhangwen, W.; Ji - Jun, J.; Yan - Zhong, F.; Shao - Ping, Z.; Chen - Chen, C.; Yu - Hao, L.; Dieter, F.; Cheng - Yong, S., Precise Modulation of the Breathing Behavior and Pore Surface in Zr - MOFs by Reversible Post - Synthetic Variable - Spacer Installation to Fine - Tune the Expansion Magnitude and Sorption Properties. *Angew. Chem. Int. Ed.* **2016**, *55*, 9932-9936.

(30) Huang, Y.-B.; Wang, Q.; Liang, J.; Wang, X.; Cao, R., Soluble Metal-Nanoparticle-Decorated Porous Coordination Polymers for the Homogenization of Heterogeneous Catalysis. *J. Am. Chem. Soc.* **2016**, *138*, 10104-10107.

(31) Cheng - Xia, C.; Shao - Ping, Z.; Zhang - Wen, W.; Chen - Chen, C.; Hai - Ping, W.; Dawei, W.; Ji - Jun, J.; Dieter, F.; Cheng - Yong, S., A Robust Metal - Organic Framework Combining Open Metal Sites and Polar Groups for Methane Purification and CO<sub>2</sub>/Fluorocarbon Capture. *Chem. Eur. J.* **2017**, *23*, 4060-4064.

(32) Yi, J.-D.; Xu, R.; Wu, Q.; Zhang, T.; Zang, K.-T.; Luo, J.; Liang, Y.-L.; Huang, Y.-B.; Cao, R., Atomically Dispersed Iron-Nitrogen Active Sites within Porphyrinic Triazine-Based Frameworks for Oxygen Reduction Reaction in Both Alkaline and Acidic Media. *ACS Energy Lett.* **2018**, *3*, 883-889.

(33) Xiao, D. J.; Bloch, E. D.; Mason, J. A.; Queen, W. L.; Hudson, M. R.; Planas, N.; Borycz, J.; Dzubak, A. L.; Verma, P.; Lee, K.; Bonino, F.; Crocellà, V.; Yano, J.; Bordiga, S.; Truhlar, D. G.; Gagliardi, L.; Brown, C. M.; Long, J. R., Oxidation of ethane to ethanol by N<sub>2</sub>O in a metal-organic framework with coordinatively unsaturated iron(II) sites. *Nat. Chem.* **2014**, *6*, 590.

(34) Zhang, T.; Manna, K.; Lin, W., Metal-Organic Frameworks Stabilize Solution-Inaccessible Cobalt Catalysts for Highly Efficient Broad-Scope Organic Transformations. *J. Am. Chem. Soc.* **2016**, *138*, 3241-3249.

(35) Metzger, E. D.; Comito, R. J.; Hendon, C. H.; Dincă, M., Mechanism of Single-Site Molecule-Like Catalytic Ethylene Dimerization in Ni-MFU-4l. *J. Am. Chem. Soc.* **2017**, *139*, 757-762.

(36) Ji, P.; Feng, X.; Veroneau, S. S.; Song, Y.; Lin, W., Trivalent Zirconium and Hafnium Metal-Organic Frameworks for Catalytic 1,4-De-aromatic Additions of Pyridines and Quinolines. *J. Am. Chem. Soc.* **2017**, *139*, 15600-15603.

(37) Yang, D.; Odoh, S. O.; Wang, T. C.; Farha, O. K.; Hupp, J. T.; Cramer, C. J.; Gagliardi, L.; Gates, B. C., Metal-Organic Framework Nodes as Nearly Ideal Supports for Molecular Catalysts: NU-1000- and UiO-66-Supported Iridium Complexes. *J. Am. Chem. Soc.* **2015**, *137*, 7391-7396.

(38) Manna, K.; Ji, P.; Greene, F. X.; Lin, W., Metal-Organic Framework Nodes Support Single-Site Magnesium-Alkyl Catalysts for Hydroboration and Hydroamination Reactions. *J. Am. Chem. Soc.* **2016**, *138*, 7488-7491.

(39) Ji, P.; Manna, K.; Lin, Z.; Feng, X.; Urban, A.; Song, Y.; Lin, W., Single-Site Cobalt Catalysts at New Zr<sub>12</sub>(μ<sub>3</sub>-O)<sub>8</sub>(μ<sub>3</sub>-OH)<sub>8</sub>(μ<sub>2</sub>-OH)<sub>6</sub> Metal-Organic Framework Nodes for Highly Active Hydrogenation of Nitroarenes, Nitriles, and Isocyanides. *J. Am. Chem. Soc.* **2017**, *139*, 7004-7011.

(40) Ji, P.; Song, Y.; Drake, T.; Veroneau, S. S.; Lin, Z.; Pan, X.; Lin, W., Titanium(III)-Oxo Clusters in a Metal-Organic Framework Support Single-Site Co(II)-Hydride Catalysts for Arene Hydrogenation. *J. Am. Chem. Soc.* **2018**, *140*, 433-440.

(41) Thierry, L.; Christian, S.; Clarisse, H.; Gerhard, F.; Francis, T.; Marc, H.; Thierry, B.; Gérard, F., A Rationale for the Large Breathing of the Porous Aluminum Terephthalate (MIL - 53) Upon Hydration. *Chem. Eur. J.* **2004**, *10*, 1373-1382.

(42) Senkovska, I.; Hoffmann, F.; Fröba, M.; Getzschmann, J.; Böhlmann, W.; Kaskel, S., New highly porous aluminium based metal-organic frameworks: Al(OH)(ndc) (ndc=2,6-naphthalene dicarboxylate) and Al(OH)(bpd) (bpd=4,4'-biphenyl dicarboxylate). *Microporous Mesoporous Mater.* **2009**, *122*, 93-98.

(43) Bloch, E. D.; Britt, D.; Lee, C.; Doonan, C. J.; Uribe-Romo, F. J.; Furukawa, H.; Long, J. R.; Yaghi, O. M., Metal Insertion in a Microporous Metal-Organic Framework Lined with 2,2'-Bipyridine. *J. Am. Chem. Soc.* **2010**, *132*, 14382-14384.

(44) Alexandra, F.; A., C. P.; P., I. C.; A., T. A.; Z., K. Y.; V., W. P.; R., D. J.; J., R. M., A Water - Stable Porphyrin - Based Metal - Organic Framework Active for Visible - Light Photocatalysis. *Angew. Chem.* **2012**, *124*, 7558-7562.

(45) Gándara, F.; Furukawa, H.; Lee, S.; Yaghi, O. M., High Methane Storage Capacity in Aluminum Metal-Organic Frameworks. *J. Am. Chem. Soc.* **2014**, *136*, 5271-5274.

(46) Larson, P. J.; Cheney, J. L.; French, A. D.; Klein, D. M.; Wylie, B. J.; Cozzolino, A. F., Anchored Aluminum Catalyzed Meerwein-Ponndorf-Verley Reduction at the Metal Nodes of Robust MOFs. *Inorg. Chem.* **2018**.

(47) Miyaura, N.; Suzuki, A., Palladium-catalyzed cross-coupling

- reactions of organoboron compounds. *Chem. Rev.* **1995**, *95*, 2457-2483.
- (48) Martin, R.; Buchwald, S. L., Palladium-Catalyzed Suzuki–Miyaura Cross-Coupling Reactions Employing Dialkylbiaryl Phosphine Ligands. *Acc. Chem. Res.* **2008**, *41*, 1461-1473.
- (49) Suzuki, A., Cross - Coupling Reactions Of Organoboranes: An Easy Way To Construct C–C Bonds (Nobel Lecture). *Angew. Chem. Int. Ed.* **2011**, *50*, 6722-6737.
- (50) Pereira, S.; Srebnik, M., Hydroboration of alkynes with pinacolborane catalyzed by HZrCp2Cl. *Organometallics* **1995**, *14*, 3127-3128.
- (51) He, X.; Hartwig, J. F., True Metal-Catalyzed Hydroboration with Titanium. *J. Am. Chem. Soc.* **1996**, *118*, 1696-1702.
- (52) Lee, T.; Baik, C.; Jung, I.; Song, K. H.; Kim, S.; Kim, D.; Kang, S. O.; Ko, J., Stereoselective Hydroboration of Diynes and Triyne to Give Products Containing Multiple Vinylene Bridges: A Versatile Application to Fluorescent Dyes and Light-Emitting Copolymers. *Organometallics* **2004**, *23*, 4569-4575.
- (53) Neilson, B. M.; Bielawski, C. W., Photoswitchable Metal-Mediated Catalysis: Remotely Tuned Alkene and Alkyne Hydroborations. *Organometallics* **2013**, *32*, 3121-3128.
- (54) Haberberger, M.; Enthaler, S., Straightforward Iron - Catalyzed Synthesis of Vinylboronates by the Hydroboration of Alkynes. *Chem. Asian J.* **2013**, *8*, 50-54.
- (55) Greenhalgh, M. D.; Thomas, S. P., Chemo-, regio-, and stereoselective iron-catalysed hydroboration of alkenes and alkynes. *Chem. Commun.* **2013**, *49*, 11230-11232.
- (56) Nakajima, K.; Kato, T.; Nishibayashi, Y., Hydroboration of Alkynes Catalyzed by Pyrrolide-Based PNP Pincer–Iron Complexes. *Org. Lett.* **2017**, *19*, 4323-4326.
- (57) Obligacion, J. V.; Neely, J. M.; Yazdani, A. N.; Pappas, I.; Chirik, P. J., Cobalt catalyzed Z-selective hydroboration of terminal alkynes and elucidation of the origin of selectivity. *J. Am. Chem. Soc.* **2015**, *137*, 5855-5858.
- (58) Ben-Daat, H.; Rock, C. L.; Flores, M.; Groy, T. L.; Bowman, A. C.; Trovitch, R. J., Hydroboration of alkynes and nitriles using an  $\alpha$ -diimine cobalt hydride catalyst. *Chem. Commun.* **2017**, *53*, 7333-7336.
- (59) Lipshutz, B. H.; Bošković, Ž. V.; Aue, D. H., Synthesis of Activated Alkenylboronates from Acetylenic Esters by CuH - Catalyzed 1, 2 - Addition/Transmetalation. *Angew. Chem.* **2008**, *120*, 10337-10340.
- (60) Semba, K.; Fujihara, T.; Terao, J.; Tsuji, Y., Copper - Catalyzed Highly Regio - and Stereoselective Directed Hydroboration of Unsymmetrical Internal Alkynes: Controlling Regioselectivity by Choice of Catalytic Species. *Chem. Eur. J.* **2012**, *18*, 4179-4184.
- (61) Bew, S. P.; Hiatt-Gipson, G. D.; Lovell, J. A.; Poullain, C., Mild reaction conditions for the terminal deuteration of alkynes. *Org. Lett.* **2012**, *14*, 456-459.
- (62) Lawrence, S. A., *Amines: synthesis, properties and applications*. Cambridge University Press: 2004.
- (63) Geri, J. B.; Szymczak, N. K., A proton-switchable bifunctional ruthenium complex that catalyzes nitrile hydroboration. *J. Am. Chem. Soc.* **2015**, *137*, 12808-12814.
- (64) Weetman, C.; Anker, M. D.; Arrowsmith, M.; Hill, M. S.; Kociok-Köhn, G.; Liptrot, D. J.; Mahon, M. F., Magnesium-catalysed nitrile hydroboration. *Chem. Sci.* **2016**, *7*, 628-641.
- (65) Kaithal, A.; Chatterjee, B.; Gunanathan, C., Ruthenium-Catalyzed Selective Hydroboration of Nitriles and Imines. *J. Org. Chem.* **2016**, *81*, 11153-11161.
- (66) Speier, J. L., Homogeneous catalysis of hydrosilylation by transition metals. In *Adv. Organomet. Chem.*, Elsevier: 1979; Vol. 17, pp 407-447.
- (67) Marciniak, B., *Hydrosilylation: a comprehensive review on recent advances*. Springer Science & Business Media: 2008; Vol. 1.
- (68) Morris, R. H., Asymmetric hydrogenation, transfer hydrogenation and hydrosilylation of ketones catalyzed by iron complexes. *Chem. Soc. Rev.* **2009**, *38*, 2282-2291.
- (69) Bhattacharya, P.; Krause, J. A.; Guan, H., Iron Hydride Complexes Bearing Phosphinite-Based Pincer Ligands: Synthesis, Reactivity, and Catalytic Application in Hydrosilylation Reactions. *Organometallics* **2011**, *30*, 4720-4729.
- (70) Albright, A.; Gawley, R. E., Application of a C2-Symmetric Copper Carbenoid in the Enantioselective Hydrosilylation of Dialkyl and Aryl–Alkyl Ketones. *J. Am. Chem. Soc.* **2011**, *133*, 19680-19683.
- (71) Yu, S.; Shen, W.; Li, Y.; Dong, Z.; Xu, Y.; Li, Q.; Zhang, J.; Gao, J., Iron - Catalyzed Highly Enantioselective Reduction of Aromatic Ketones with Chiral P2N4 - Type Macrocycles. *Adv. Synth. Catal.* **2012**, *354*, 818-822.
- (72) MacMillan, S. N.; Harman, W. H.; Peters, J. C., Facile Si–H bond activation and hydrosilylation catalysis mediated by a nickel–borane complex. *Chem. Sci.* **2014**, *5*, 590-597.
- (73) Zhou, H.; Sun, H.; Zhang, S.; Li, X., Synthesis and Reactivity of a Hydrido CNC Pincer Cobalt(III) Complex and Its Application in Hydrosilylation of Aldehydes and Ketones. *Organometallics* **2015**, *34*, 1479-1486.
- (74) Bezier, D.; Venkanna, G. T.; Castro, L. C. M.; Zheng, J.; Roisnel, T.; Sortais, J. B.; Darcel, C., Iron - Catalyzed Hydrosilylation of Esters. *Adv. Synth. Catal.* **2012**, *354*, 1879-1884.
- (75) Mukhopadhyay, T. K.; Flores, M.; Groy, T. L.; Trovitch, R. J., A highly active manganese precatalyst for the hydrosilylation of ketones and esters. *J. Am. Chem. Soc.* **2014**, *136*, 882-885.
- (76) Kovalenko, O. O.; Adolfsson, H., Highly Efficient and Chemoselective Zinc - Catalyzed Hydrosilylation of Esters under Mild Conditions. *Chem. Eur. J.* **2015**, *21*, 2785-2788.
- (77) Gephart, R. T.; Warren, T. H., Copper-Catalyzed sp<sup>3</sup> C–H Amination. *Organometallics* **2012**, *31*, 7728-7752.
- (78) Roizen, J. L.; Harvey, M. E.; Du Bois, J., Metal-Catalyzed Nitrogen-Atom Transfer Methods for the Oxidation of Aliphatic C–H Bonds. *Acc. Chem. Res.* **2012**, *45*, 911-922.
- (79) Park, Y.; Kim, Y.; Chang, S., Transition Metal-Catalyzed C–H Amination: Scope, Mechanism, and Applications. *Chem. Rev.* **2017**, *117*, 9247-9301.
- (80) Jang, E. S.; McMullin, C. L.; Käb, M.; Meyer, K.; Cundari, T. R.; Warren, T. H., Copper(II) Anilides in sp<sup>3</sup> C–H Amination. *J. Am. Chem. Soc.* **2014**, *136*, 10930-10940.
- (81) Tran, B. L.; Li, B.; Driess, M.; Hartwig, J. F., Copper-Catalyzed Intermolecular Amidation and Imidation of Unactivated Alkanes. *J. Am. Chem. Soc.* **2014**, *136*, 2555-2563.
- (82) Tsuji, J., Synthetic Applications of the Palladium-Catalyzed Oxidation of Olefins to Ketones. *Synthesis* **1984**, *1984*, 369-384.
- (83) Reinhard, J., Acetaldehyde from Ethylene—A Retrospective on the Discovery of the Wacker Process. *Angew. Chem. Int. Ed.* **2009**, *48*, 9034-9037.
- (84) Jia, D. J.; R., B. W.; L., F. B., Palladium - Catalyzed anti - Markovnikov Oxidation of Terminal Alkenes. *Angew. Chem. Int. Ed.* **2015**, *54*, 734-744.
- (85) Baiju, T. V.; Gravel, E.; Doris, E.; Namboothiri, I. N. N., Recent developments in Tsuji-Wacker oxidation. *Tetrahedron Lett.* **2016**, *57*, 3993-4000.
- (86) Chaudhari, D. A.; Fernandes, R. A., Hypervalent Iodine as a Terminal Oxidant in Wacker-Type Oxidation of Terminal Olefins to Methyl Ketones. *J. Org. Chem.* **2016**, *81*, 2113-2121.
- (87) Teo, P.; Wickens, Z. K.; Dong, G.; Grubbs, R. H., Efficient and Highly Aldehyde Selective Wacker Oxidation. *Org. Lett.* **2012**, *14*, 3237-3239.

1 (88) Bill, M.; K., W. Z.; H., G. R., Regioselective Wacker  
2 Oxidation of Internal Alkenes: Rapid Access to Functionalized  
3 Ketones Facilitated by Cross - Metathesis. *Angew. Chem.* **2013**,  
4 *125*, 9933-9936.  
5 (89) Liu, B.; Jin, F.; Wang, T.; Yuan, X.; Han, W., Wacker - Type  
6 Oxidation Using an Iron Catalyst and Ambient Air: Application to  
7  
8  
9  
10  
11  
12  
13  
14  
15  
16  
17  
18  
19  
20  
21  
22  
23  
24  
25  
26  
27  
28  
29  
30  
31  
32  
33  
34  
35  
36  
37  
38  
39  
40  
41  
42  
43  
44  
45  
46  
47  
48  
49  
50  
51  
52  
53  
54  
55  
56  
57  
58  
59  
60

Late - Stage Oxidation of Complex Molecules. *Angew. Chem. Int.*  
*Ed.* **2017**, *56*, 12712-12717.

TOC:

